Electronic Supplementary Material (ESM)

In situ synthesis and characterization of sulfonic acid functionalized hierarchical silica monoliths

Richard Kohns[1,2], Ralf Meyer[2], Marianne Wenzel[3], Jörg Matysik[3], Dirk Enke[2] and Ulrich Tallarek*[1]

[1] Department of Chemistry, Philipps-Universität Marburg, Hans-Meerwein-Strasse 4, 35032 Marburg, Germany

[2] Institute of Chemical Technology, Universität Leipzig, Linnéstrasse 3, 04103 Leipzig, Germany

[3] Institute of Analytical Chemistry, Universität Leipzig, Linnéstrasse 3, 04103 Leipzig, Germany

---

* Corresponding author.
Fax: +49-(0)6421-28-27061, E-mail: tallarek@staff.uni-marburg.de.
https://orcid.org/0000-0002-2826-2833.

Table S1 Starting compositions of the in situ functionalized sol–gel silica monoliths

Sample	*m* (H_2O) / g	*m* (Urea) / g	*m* (PEO) / g	*m* (H_2SO_4) / g	*m* (TEOS) / g	*m* (MPTMS) / g
P-1.5-S-1	18.0	2.40	1.50	1.26	13.6	1.06
P-1.6-S-1	18.0	2.40	1.60	1.26	13.6	1.06
P-1.7-S-1	18.0	2.40	1.70	1.26	13.6	1.06
P-1.8-S-1	18.0	2.40	1.80	1.26	13.6	1.06
P-1.7-S-1.5	18.0	2.40	1.70	1.26	13.2	1.59
P-1.8-S-2	18.0	2.40	1.80	1.26	12.7	2.11
P-1.7-S-0	18.0	2.40	1.70	1.26	14.6	–

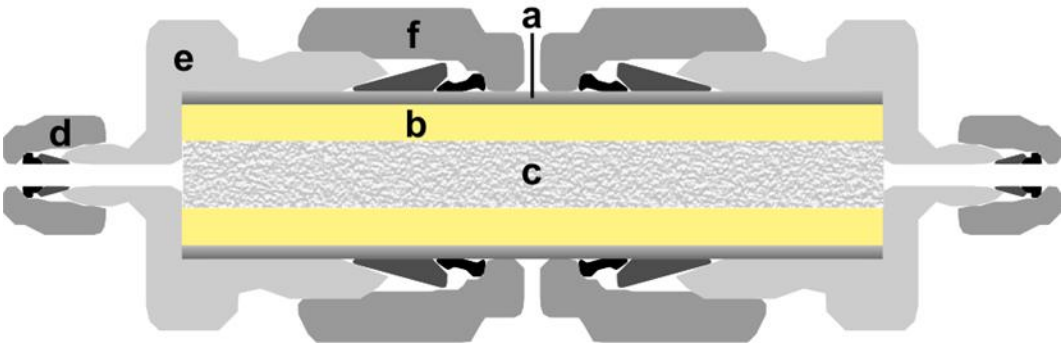

Fig. S1 Schematic drawing of the constructed column set-up [1]. (a) 1/2" o.d. stainless-steel tube (10.6 mm i.d. × 5 cm length), (b) UHU® PLUS 300 epoxy resin adhesive, (c) monolithic silica rod (5 mm i.d. × 5 cm length), (d) 5/16" nut hex with 1/16" o.d. tube, (e) 13/16" body hex, and (f) 7/8" nut hex with 1/2" o.d. tube

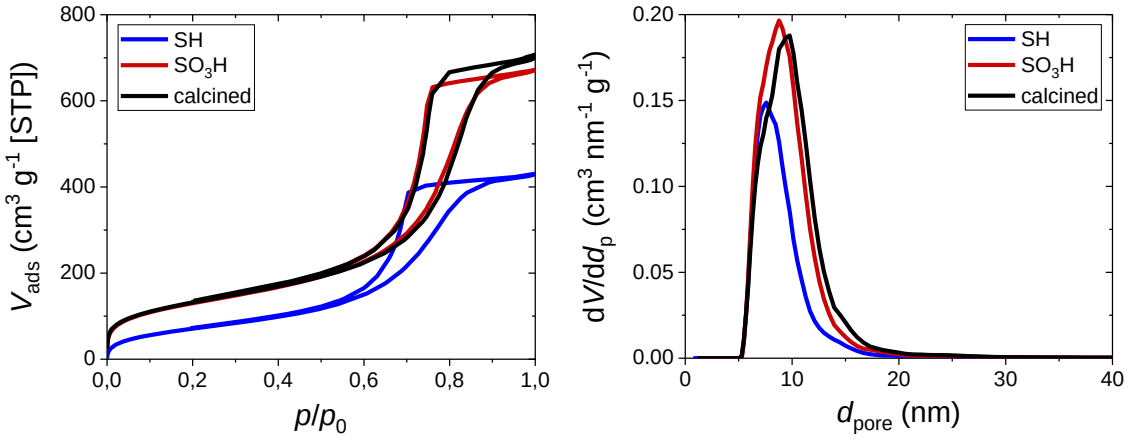

Fig. S2 Nitrogen physisorption isotherms (left) and pore size distributions (right) for sample P-1.7-S-1 in its respective modification: pristine (blue), oxidized/extracted (red) and calcined (black)

Table S2 Influence of the extraction/oxidation step on the pore space properties as verified by nitrogen physisorption analysis

Sample	d_{meso} / nm			S_{BET} / m^2 g^{-1}		
	SH[a]	SO_3H	calc.	SH[a]	SO_3H	calc.
P-1.7-S-1	8	9	10	273	469	479
P-1.7-S-0	26	–	26	167	–	195

[a] The SH modification in the case of the reference material P-1.7-S-0 refers to the pure silica with the polymer still present.

Table S3 Elemental analysis before and after hydrothermal treatment

Sample	before			after		
	C / %	H / %	S / %	C / %	H / %	S / %
P-1.5-S-1	15.6	3.0	2.5	13.9	2.6	2.8
P-1.6-S-1	16.5	3.1	2.5	14.9	2.8	2.8
P-1.7-S-1	17.0	3.3	2.6	15.6	2.9	2.8
P-1.8-S-1	17.3	3.3	2.5	14.8	2.7	2.8

Table S4 Efficiency of the extraction procedure. Comparison of reference material P-1.7-S-0 with the in situ functionalized sample P-1.7-S-1 based on elemental analysis

Sample	reference			functionalized		
	C / %	H / %	S / %	C / %	H / %	S / %
P-1.7 (reference)	3.5	0.8	0.0	14.1	2.5	2.8
P-1.7_ext(2h)	1.1	0.7	0.0	3.9	1.5	2.8
P-1.7_ext(4h)	0.9	0.6	0.0	3.4	1.4	2.5
P-1.7_ext(6h)	0.8	0.6	0.0	2.9	1.3	2.0
P-1.7_ext(2h)-c	0.3	0.0	0.0	0.4	0.2	0.0
P-1.7_ext(4h)-c	0.1	0.0	0.0	0.1	0.0	0.0

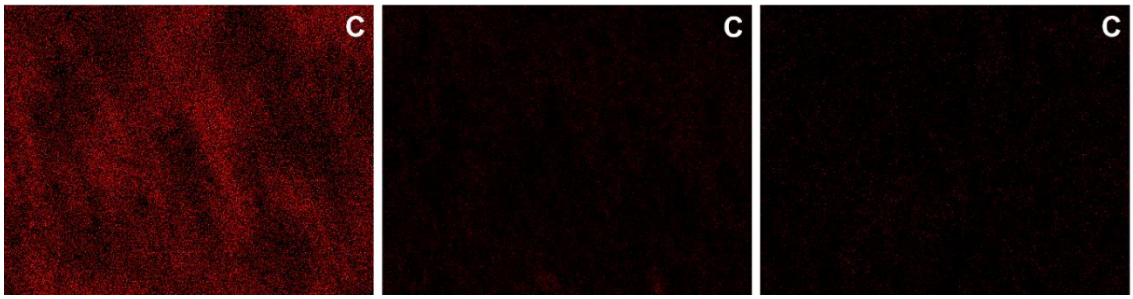

Fig. S3 SEM-EDX images of the reference material P-1.7-S-0 in its respective modification: pristine (left), extracted (middle) and calcined (right)

The untreated pristine sample consists of 11 at.% (7.2 wt.%) C, 0.2 at.% (0.3 wt.%) S, 59 at.% (50 wt.%) O and 28 at.% (42 wt.%) Si (rounded values). After the extraction step, the detected composition of the sample is 1 at.% (0.6 wt.%) C, 0.2 at.% (0.3 wt.%) S, 61 at.% (48 wt.%) O and 36 at.% (50 wt.%) Si. Compared to the extracted sample, the calcined material has the same composition: 1 at.% (0.5 wt.%) C, 0.2 at.% (0.3 wt.%) S, 61 at.% (48 wt.%) O and 36 at.% (49 wt.%) Si.

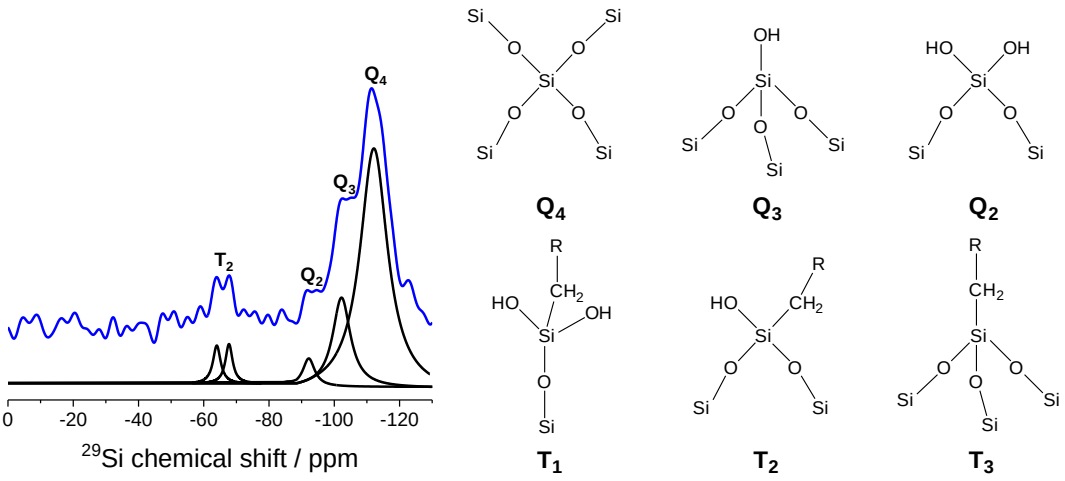

Fig. S4 Integrated HPDEC/MAS ^{29}Si NMR spectrum of the pristine sample P-1.7-S-1 (before the extraction step) and terminology for the silicon species

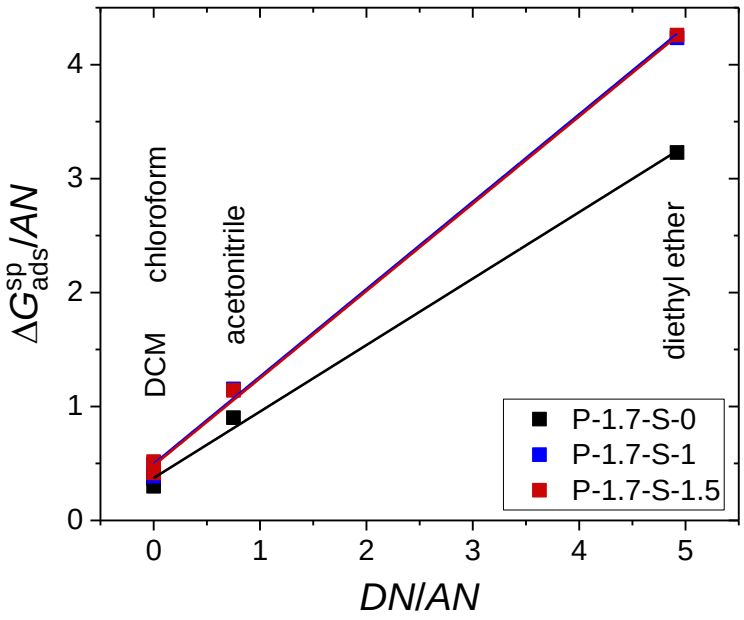

Fig. S5 Determination of the Lewis acid-base parameters K_A and K_D for the surfaces of non-functionalized (P-1.7-S-0) and sulfonic acid functionalized silica monoliths with different SO_3H loadings (P-1.7-S-1 and P-1.7-S-1.5) using Gutmann's approach (Eq. S1)

The Lewis-acid parameter K_A is given by the slope of the linearized Gutmann plot, whereas the intercept with the vertical axis provides the Lewis-base parameter K_D:

$$\frac{\Delta G_{ads}^{sp}}{AN} = K_A \frac{DN}{AN} + K_D \qquad \text{(S1)}$$

Determination of the total surface energy

The total surface energy γ_s^t has a dispersive (γ_s^d) and a specific (γ_s^{sp}) component. The dispersive component can be determined under IGC conditions of infinite dilution using *n*-alkane probe molecules, which then adsorb completely flat on the surface. The longer the hydrocarbon chain, the stronger the dispersive (also known as Lifshitz–van der Waals) interactions. The retention time t_N obtained with constant carrier-gas flow $\dot{V}$ is a measure for the work of adhesion of the probe molecules and can be expressed by the retention volume V_N. Graphically, it is described as the volume necessary to purge the probe molecules from the column with respect to their individual adsorption-desorption equilibrium

$$V_N = \dot{V} j \left(\frac{T}{273.15\ \text{K}}\right) t_N \qquad \text{(S2)}$$

where T denotes temperature and j the James–Martin mobile phase compressibility correction factor [2]. The retention volume V_N from Eq. S2 is used to calculate the free energy of adsorption ΔG_{ads} expressed as

$$\Delta G_{\mathrm{ads}} = -RT \ln(V_{\mathrm{N}}) + C \tag{S3}$$

where R is the universal gas constant and C is a constant that depends on a reference state for the adsorbed molecules (usually neglected in the determination of the free adsorption enthalpy). The slope of the *n*-alkane reference line (Fig. 6), which characterizes the dependence of the free energy of adsorption on the number of CH_2 groups (the free energy of adsorption varies linearly with the number of carbon atoms [3,4]) provides the dispersive component of the surface energy (γ_s^d) after using Eq. S4

$$\gamma_{\mathrm{s}}^{\mathrm{d}} = \frac{[\Delta G_{\mathrm{ads}}(\mathrm{CH_2})]^2}{4\, N_{\mathrm{A}}^2\, (a_{\mathrm{CH_2}})\, \gamma_{\mathrm{CH_2}}} \tag{S4}$$

where a_{CH_2} is the area of a methylene unit, N_A is Avogadro's constant and γ_{CH_2} is the surface energy of a solid based only on methylene units, *i.e.*, polyethylene.

The specific component of the surface energy can be calculated from interactions of polar probe molecules with the solid surface. These interactions have both specific (polar) and dispersive character. Therefore, as proposed by Donnet *et al.* [5], the specific interaction parameter (ΔG_{ads}^{sp}) is determined by the difference between the free enthalpies of adsorption for the polar molecule (ΔG_{ads}) and the hypothetical or real *n*-alkane with the same topological index χ_T (ΔG_{ads}^{d}), which can be expressed as follows:

$$\Delta G_{\mathrm{ads}}^{\mathrm{sp}} = \Delta G_{\mathrm{ads}} - \Delta G_{\mathrm{ads}}^{\mathrm{d}} \tag{S5}$$

The specific component of the surface energy (γ_s^{sp}) results from ΔG_{ads}^{sp} by applying the Van Oss theory [6], leading to Eq. S6

$$\Delta G_{\mathrm{ads}}^{\mathrm{sp}} = 2 a_{\mathrm{l}} N_{\mathrm{A}} \left(\sqrt{\gamma_{\mathrm{l}}^{+}\, \gamma_{\mathrm{s}}^{-}} + \sqrt{\gamma_{\mathrm{l}}^{-}\, \gamma_{\mathrm{s}}^{+}}\right) \tag{S6}$$

where a_l is the cross-sectional area, γ_l^+ the Lewis-donor parameter and γ_l^- the Lewis-acceptor parameter of the probe molecule. The Lewis-acid (electron acceptor) parameter γ_s^+ and the Lewis-base (electron donor) parameter γ_s^- of the solid surface can be obtained with a nonlinear parameter approach presented in Bauer *et al*. [7]. The calculation of γ_s^{sp} follows from Eq. S7

using both the Lewis-acid and the Lewis-base parameter and provides results in the same unit as the surface energy [8]

$$\gamma_s^{sp} = 2\sqrt{\gamma_s^+ \gamma_s^-} \quad \text{(S7)}$$

Finally, from the measured data, the resulting dispersive and specific components of the surface energy can be summed up, giving the total surface energy of the solid under study, as expressed by Eq. S8 (Table 4):

$$\gamma_s^t = \gamma_s^d + \gamma_s^{sp} \quad \text{(S8)}$$

References

1. Kohns R, Haas CP, Höltzel A, Splith C, Enke D, Tallarek U (2018) Hierarchical silica monoliths with submicron macropores as continuous-flow microreactors for reaction kinetic and mechanistic studies in heterogeneous catalysis. React Chem Eng 3:353–364.
2. James AT, Martin AJP (1952) Gas-liquid partition chromatography: the separation and micro-estimation of volatile fatty acids from formic acid to dodecanoic acid. Biochem J 50:679–690.
3. Dorris GM, Gray DG (1980) Adsorption of *n*-alkanes at zero surface coverage on cellulose paper and wood fibers. J Colloid Interface Sci 77:353–362.
4. Shi B, Wang Y, Jia L (2011) Comparison of Dorris-Gray and Schultz methods for the calculation of surface dispersive free energy by inverse gas chromatography. J Chromatogr A 1218:860–862.
5. Donnet JB, Park SJ, Balard H (1991) Evaluation of specific interactions of solid surfaces by inverse gas chromatography. Chromatographia 31:434–440.
6. Van Oss CJ, Chaudhury MK, Good RJ (1987) Monopolar surfaces. Adv Colloid Interface Sci 28:35–64.
7. Bauer F, Meyer R, Czihal S, Bertmer M, Decker U, Naumov S, Uhlig H, Steinhart M, Enke D (2019) Functionalization of porous siliceous materials, Part 2: Surface characterization by inverse gas chromatography. J Chromatogr A 1603:297–310.
8. Van Oss CJ, Good RJ, Chaudhury MK (1988) Additive and nonadditive surface tension compounds and the interpretation of contact angles. Langmuir 4:884–891.